In Situ Observations of Annealing Behavior of Polyethylene Single Crystals on Various Substrates by AFM

Junichi Nakamura and Akiyoshi Kawaguchi*

Faculty of Science and Engineering, Ritsumeikan University, Nojihigashi 1-1-1, Kusatsu, Shiga 525−8577, Japan

Received January 19, 2004; Revised Manuscript Received March 12, 2004

ABSTRACT: Polyethylene single crystals were annealed on various kinds of substrates: a glass plate, evaporated Pt/Pd, evaporated amorphous carbon, HOPG (highly organized pyrolytic graphite), and uniaxially oriented isotactic polypropylene (iPP). Their morphological changes on these substrates by annealing were observed in situ by AFM. On glass and Pt/Pd substrates, polyethylene single crystals started reorganizing from the periphery, accompanying thickening of lamellae, and eventually became molten. Polyethylene single crystals behaved quite differently between on amorphous carbon and on HOPG, which both had the identical chemical constitution: on HOPG, fibrils were produced, extending radially from the center of polyethylene single crystals, while on amorphous carbon, lamellae thickened and melted down without forming any peculiar texture. This difference was caused by the difference in atomic array between the surfaces of HOPG and amorphous carbon. On oriented iPP, a fibrillar texture, with the long axis of fibrils oriented at an angle of 40° with the iPP fiber axis, was formed in the process of slow heating. The oriented fibrillar textures that were produced on HOPG and iPP in the heating process were formed under epitaxial control of the surface structure of substrate. The present work showed that *oriented crystallization occurred through partial melting in the process of annealing.*

Introduction

Since solution-grown polyethylene single crystals were first found, there has been much interest in the phenomenon of the lamellar thickness of polymer crystals increasing by annealing. A vast number of works on annealing of polymer single crystals have been done, although mainly on polyethylene single crystals, using various methods, such as optical and electron microscopy, X-ray and neutron diffraction, infrared spectroscopy, DSC, and NMR, as we can see from early papers,[1,2] reviews,[3] and monographs.[4−6] Of the annealing behaviors, the dependence of lamellar thickness on annealing temperature and annealing time was investigated intensively and extensively not only from academic interest but also from practical viewpoints, because heat treatment is an important procedure to improve the physical properties of polymer products. The time dependence of lamellar thickness by annealing was first theoretically treated by N. Hirai et al.,[7] and the log *t* law was established.[7,8] Studies on morphological or structural changes by annealing were also carried out to understand its effect on the physical properties of polymers. Transmission electron microscopy revealed that morphological changes given rise to by heat treatment depend on the annealing temperature[9] and annealing time.[10] It is well-known, for example, that when polymer single crystals are annealed on a substrate, holes are produced all over the whole area, and their formation accompanies lamellar thickening. However, the following two points have not been paid attention to in the annealing experiments done so far: (1) How does the morphology of polymer crystals change with annealing time?[10] (2) How is the morphology of polymer crystals influenced by the kind of substrate on annealing? For example, annealing of single crystals mats and bulk materials corresponds to the case on or between the substrates of the same kind of polymer.

Atomic force microscopy (AFM) is a very powerful tool for investigating the morphology of polymer crystals, although limited to the observation of surface morphology. Using AFM, morphology and structure of polyethylene single crystals have been observed,[11−20] even at the molecular level.[21] Their morphology and annealing behavior have been further elucidated through the AFM results, complementing the electron microscopic works. Recently, AFM has been developed technically to enable observing, in situ and in real time, the structural changes in the transient processes, e.g., the crystallization of polymers at high temperatures.[22−26] In particular, an in situ AFM study at high temperatures on the ultralong chain alkane $C_{390}H_{782}$ by Magonov et al.[27] provides deep insight into the annealing behavior of polyethylene crystals. Here, using the AFM method, annealing behaviors of polyethylene single crystals were followed in situ at high temperatures, focusing on the morphological changes. Further, aiming to clarify the effect of substrate on annealing behavior of polyethylene single crystals, in situ experiments were carried out on various kinds of substrates.

Experimental Section

Polyethylene single crystals were prepared by the self-seeding method,[28] using a fractionated polyethylene with M_n = 32 000 (M_w/M_n = 1.1) (No. 1483 product by NIST). Polyethylene was dissolved at a concentration of 0.05 wt % in *p*-xylene in a test tube. After crystallization at 82 °C, the test tube containing PE crystals in suspension was heated to 97 °C by transferring to an oil bath, which was controlled at the temperature. After keeping it at the temperature for a few minutes, the test tube was returned to the oil bath at 82 °C to crystallize. Polyethylene single crystals thus prepared were examined without filtration as prepared.

Annealing of these crystals was carried out on the following different kinds of substrates: a normal slide glass, evaporated

* To whom correspondence should be addressed. Fax +81-(0)-77-561-2659. E-mail akiyoshi@se.ritsumei.ac.jp.

10.1021/ma0498666 CCC: $27.50
Published on Web 04/22/2004

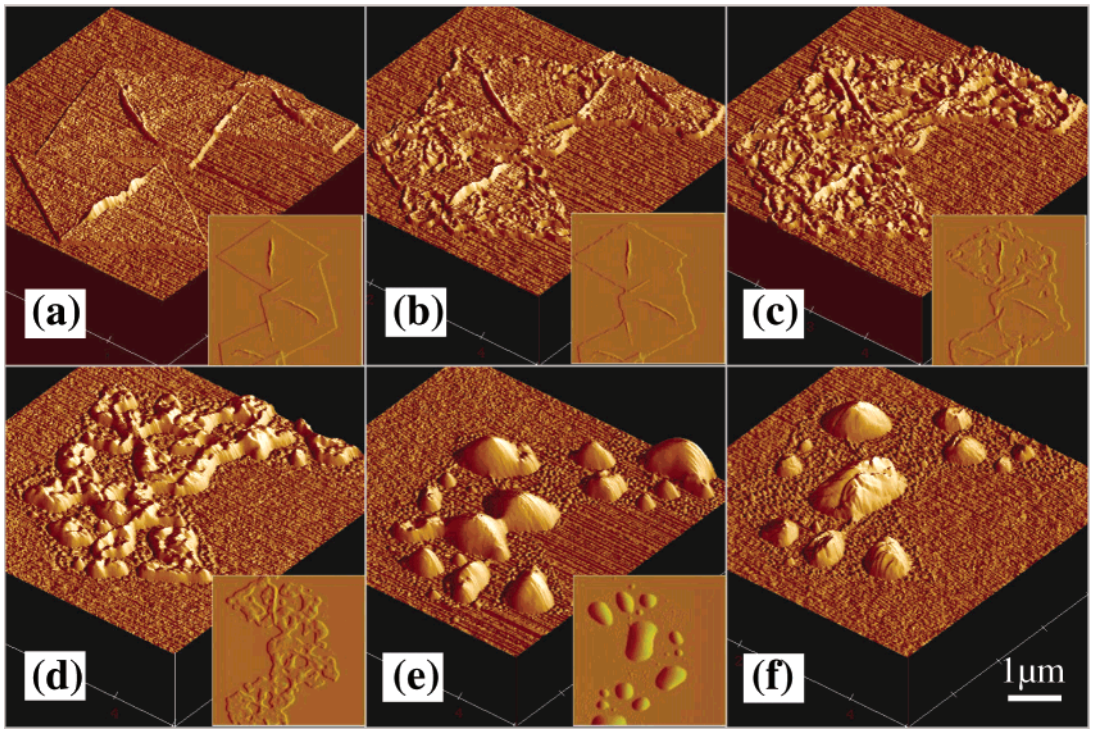

Figure 1. Landscape view of AFM height images taken in situ on annealing of polyethylene single crystals on glass plate at (a) room temperature, (b) 126, (c) 128, (d) 136, and (e) 140 °C, and (f) room temperature after being cooled from 150 °C, respectively. The inset images are the corresponding amplitude image, which show the projected patterns. All images were taken at 30 min after the specimen was heated to each temperature.

Pt/Pd, evaporated carbon film, HOPG (highly organized pyrolytic graphite) used for STM studies, and uniaxially oriented, thin isotactic polypropylene (iPP) film. An amorphous carbon film was prepared by the evaporation method, which is usually used to make a thin supporting carbon film for electron microscopy. A Pt/Pd substrate was also prepared by coating a slide glass with Pt/Pd by the evaporation method. The oriented iPP film was prepared using the Gohil and Petermann method.[29]

Polyethylene single crystals were put on the various kinds of substrates, and their morphology was observed in situ, by changing annealing temperatures, with an AFM Nanoscope IIIa, which was equipped with a heating module. It took about 5 min to take a frame of image.

Results

On annealing, the morphology of polyethylene single crystals varied quite differently depending on the kind of substrate. AFM recorded, in situ, their morphology in height, amplitude, and phase modes, simultaneously, during annealing. Only AFM images suitable to the stressed points of discussion are selected here. The annealing behaviors on various kinds of substrates are detailed below using these image data, focusing on the morphological changes.

A. On Normal Glass Plate. Figure 1 shows a series of AFM height images of polyethylene single crystals, taken in situ at various temperatures on annealing on a normal glass plate (a slide glass for optical microscopy). Figure 1b shows the meandered rim. From the height images, the thickness of polyethylene lamellae was measured. Figure 2 shows the changes in thickness at the rim of and inside a lamella as a function of annealing temperature.[17,26,27] In the narrow temperature range of about 120 to 126 °C, thickness is larger at the periphery than inside. This can be explained by that, in the narrow temperature range, lamellar thickening progresses ahead at the periphery, where the

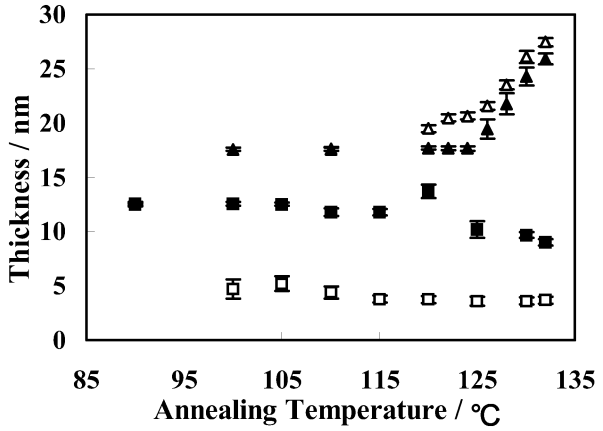

Figure 2. Lamellar thickness against the annealing temperature, i.e., the observation temperature. Marks △ and ▲ denote the thickness at the periphery and inside of lamellae on a glass plate, respectively, and □ and ■ those on HOPG surface, respectively. Here, data for glass (marks △ and ▲) are shifted upward by 5 nm to avoid confusion.

meandering morphological changes occurred. As a result, the single crystals changed morphologically, featuring a framelike structure (Figure 1b), although its feature was not as distinguished as in the case of annealing in solution.[1,2,10] It was reported that the lamellar thickening begins at about 110 °C, depending on initial thickness.[30] In the present work, it seems that observable thickening began at a rather high temperature. It is to be stressed here that the morphological changes initiate from the periphery, where thickening occurs, and subsequently occur at random inside (see also Figure 11a). Figure 1c shows that rather large holes are formed randomly over the whole lamella, and that the thickened lamella does not move out across the lozenge rim of the original lamella. By heating further,

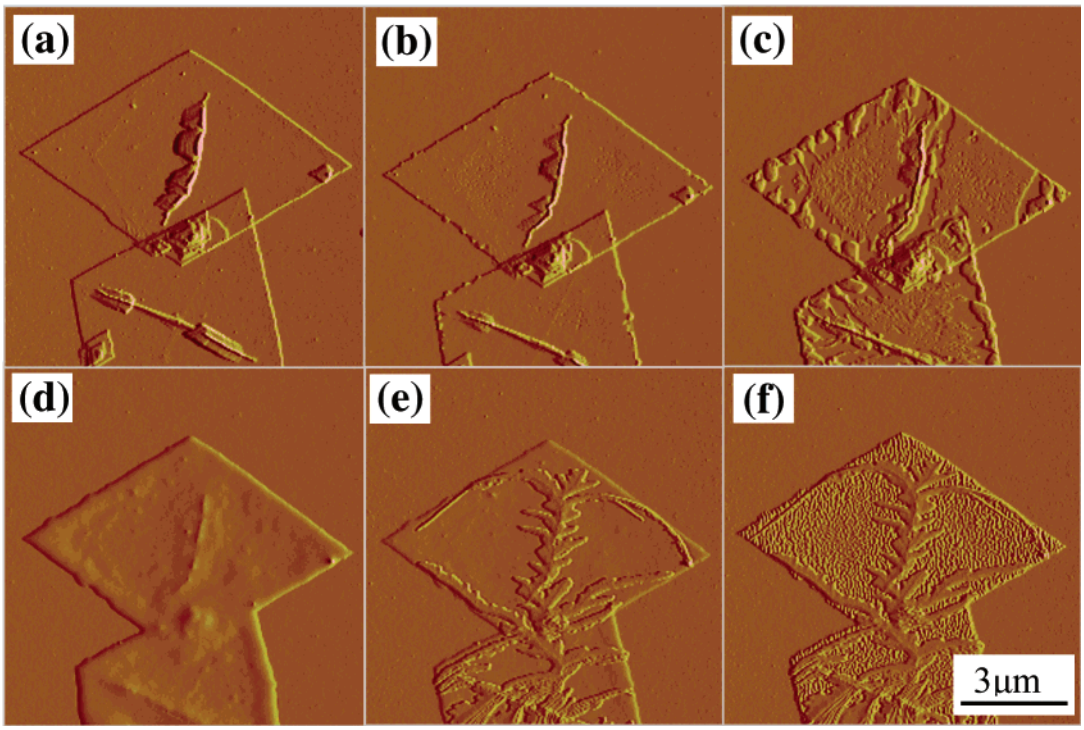

Figure 3. AFM amplitude images taken in situ on annealing of polyethylene single crystals on evaporated Pt/Pd at (a) room temperature, at (b) 132, (c) 134, and (d) 150 °C in the heating process, respectively, and at (e) 128 °C and (f) room temperature in the cooling process from 150 °C. The images were taken at 30 min after the specimen was heated to each temperature.

polyethylene lamellae were largely deformed morphologically (Figure 1d), and eventually they were melted into droplets (Figure 1e). It is found that the melt droplets are on a thin lozenge layer, the rim of which contours the original lozenge of single crystals. From the height image, the height of the lozenge layer was measured at about 1 nm. As there was no polyethylene in the open area surrounding the original polyethylene single crystals, it is certain the layer consisted of polyethylene. When the specimen was cooled from the molten state, lamellae grew within the droplets, and small globules became more conspicuous on the thin layer (see Figure 1f).

B. On Evaporated Pt/Pd Surface. Figure 3 shows a series of AFM amplitude images of polyethylene single crystals, which were taken in situ at various temperatures in the cycle of heating and cooling on the Pt/Pd substrate. In the heating process, the temperature was increased stepwise. Here, the morphological changes initiated again at the periphery. However, we see, from Figure 3c, that thickening did not evenly take place along the rim of lozenge-shaped single crystal, but that the islands morphology was formed along the rim. The islands morphology became marked with increasing temperature up to about 138 °C. However, the original lozenge shape can be retraced by contouring the rim of a thicker layer, the rim of single crystals does not meander, and the melt remains within the lozenge area at temperatures above the melting point, without condensing into droplets; compare Figure 1e and Figure 3d. The pockmarked surface with small holes in the lamellar interior, as seen in Figure 3c, disappeared in the heating process before melting, and as a result, the lozenge surface was smooth. It is characteristic that, on a Pt/Pd substrate, the molten polyethylene did not spread away across the lozenge rim of the original polyethylene single crystal.

Figure 3e shows the morphology that was formed by crystallization on cooling from the melt. A treelike coarse texture appeared along the rim of the lozenge and the short axis (the *b* axis) of the original single crystal. Even at the stage where such a coarse texture formed, the inside area was still smooth. On further cooling, small globules grew over the smooth inside area.

Parts a−c of Figure 4 show the AFM height images, the amplitude images of which correspond to parts a, d, and f of Figure 3, respectively. The corresponding height profiles were obtained by scanning along the lines in the height images. Figure 4a shows that the thickness of the original single crystal was almost uniform all over the lamella, except for the central pleat with a thickness of 90 nm. In the height profile in Figure 4b, the periphery is high in the form of a bump, and the height decreases gradually toward the inside. Polyethylene melt condensed near the rim but did not spread outward across there. It is to be noted that the inside area is still higher than the substrate level. The height is about 5 nm. In some cases, the polyethylene melt evenly covered the substrate surface with no thick edge, not spreading across the rim. Figure 4c shows a rippled profile, which reflects the fine structure of crystallized polyethylene on the Pt/Pd substrate (cf. Figure 3f).

C. On Amorphous Carbon. Polyethylene single crystals were annealed on the evaporated carbon film by increasing the temperature stepwise. Figure 5 shows a series of AFM amplitude images taken in situ at various temperatures in the process. Polyethylene single crystals were varied morphologically in the same way as on the glass plate, exhibiting a framelike feature. In contrast to a glass, the morphological changes proceeded from the periphery in.

Wedgelike notches were generated along the periphery and developed to carve into the lamellar interior,

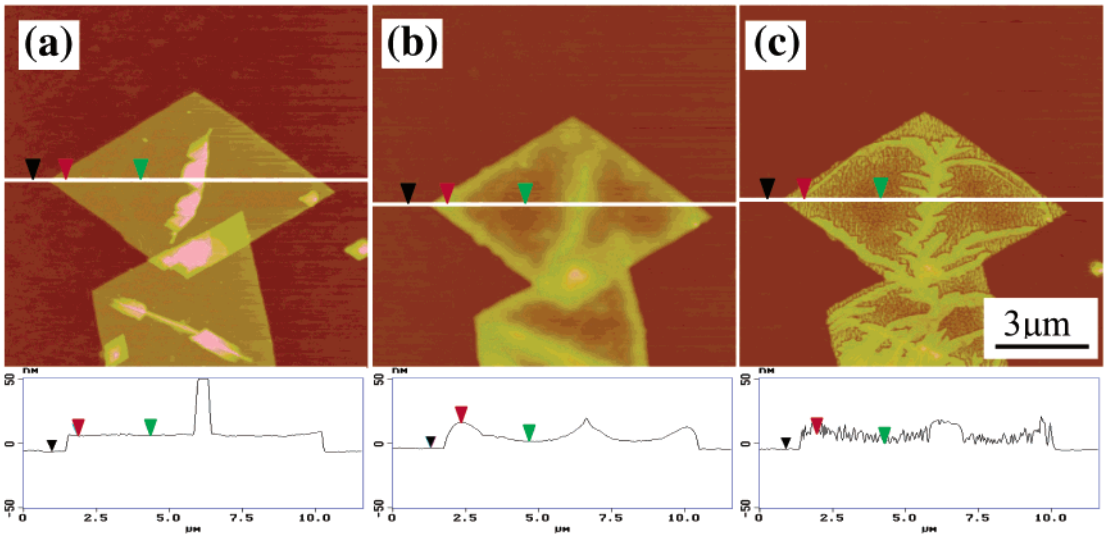

Figure 4. AFM height images taken in situ at various temperatures on annealing polyethylene single crystals on evaporated Pt/Pd at (a) room temperature, (b) 150 °C, and (c) room temperature after being cooled from 150 °C. Height profiles were obtained by scanning along the lines in the AFM images.

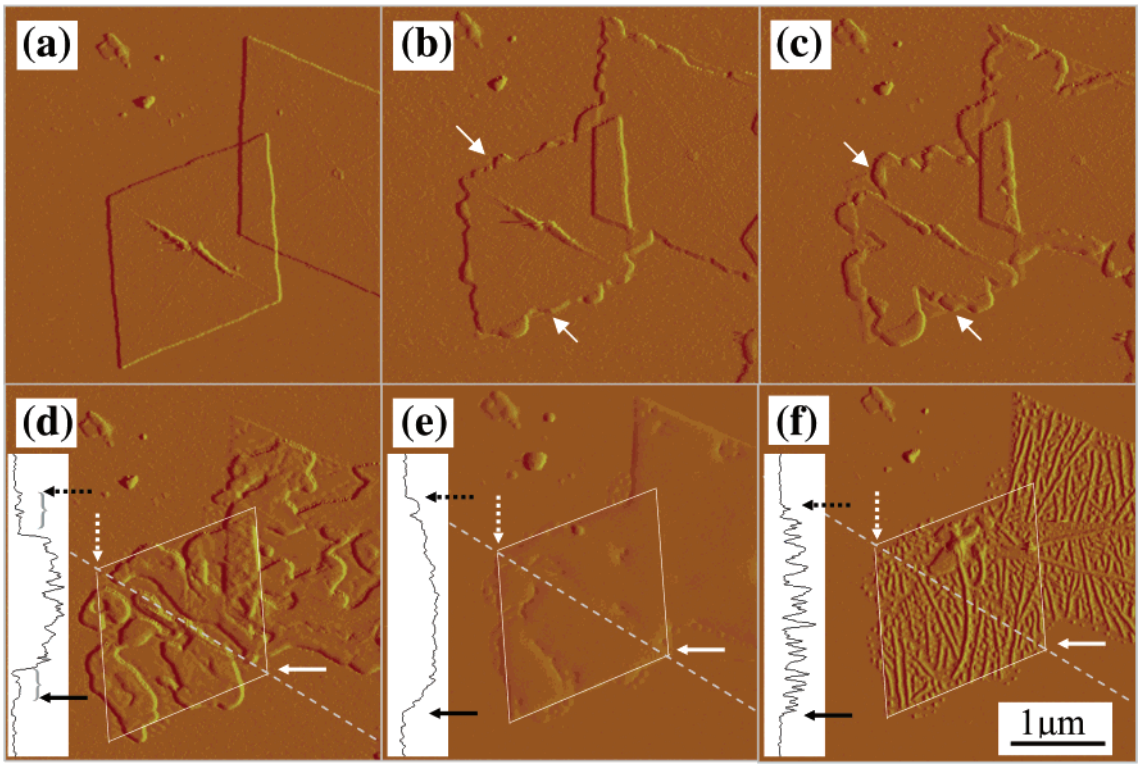

Figure 5. AFM amplitude images taken in situ at various temperatures on annealing of polyethylene single crystals on an evaporated carbon film: (a) room temperature, (b) 132, (c) 134, (d) 136, and (e) 150 °C and (f) room temperature after being cooled from 150 °C. Inset height profiles in parts d−f were obtained by scanning along the white lines in the images. Upper and lower arrows in the profile correspond to the left and right arrows in the corresponding image, which are put at the edges of the lozenge of original single crystal, respectively. The profile in part d is higher by about 1 nm from the substrate on both sides (note parts marked with a brace). This indicates the thickness of the underlying sheet layer.

with increasing of the temperature (see arrows in Figure 5, parts b and c). The lozenge single crystals were fragmented in patches into "islands and peninsulas" by deeply carved notches, as seen in Figure 5d, and they thickened as the notches were carved.[10,27] The thickened lamellae extended over the substrate surface, exceeding the rim of the original single crystals; an amoeba-like morphology resulted as seen on collodion.[7,31] The molten polyethylene droplets moved on the carbon substrate to spread over the substrate across the rim of the original lamellar lozenge (Figure 5, parts d and e). Thus, by heat treatment, the polyethylene single crystals behaved in a morphologically different manner from the behavior on a glass plate and Pt/Pd. Figure 5f shows the morphology formed in cooling from the molten state. Rodlike and globular crystallites were formed. In images of Figure 5, parts d−f, there is a thin base of lozenge shape with the thickness of about 1 nm, on which polyethylene crystals and melt stayed. The structural features of the thin base sheet are unclear.

D. On HOPG. Figure 6 shows a series of phase AFM images that were taken in situ at various temperatures

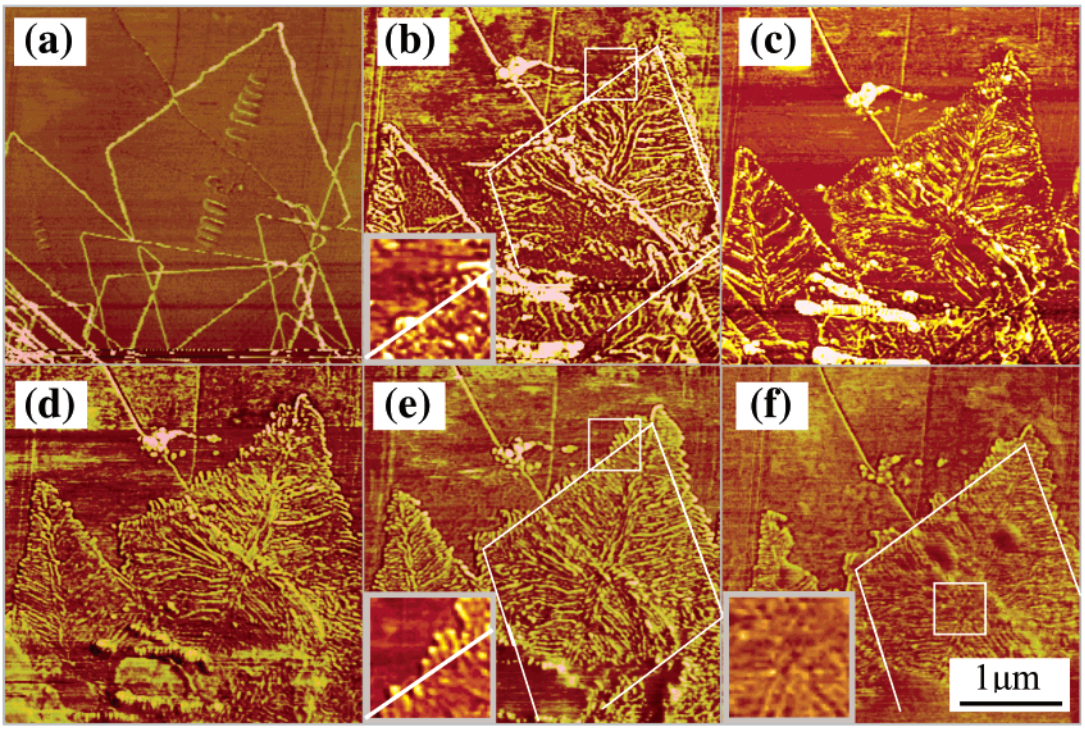

Figure 6. AFM phase images taken in situ on annealing of polyethylene single crystals on HOPG at (a) room temperature and at (b) 120, (c) 124, (d) 132, (e) 134, and (f) 138 °C. The {100} sectors are seen in part a, narrowing toward the tip along the *a* axis. Nuclei formed by self-seeding at a high temperature of 90 °C may be truncated. When crystals grow further from such truncated nuclei under the different conditions, e.g. at a lower temperature as 85 °C[1] or in the different solvent from the solvent in which nuclei were formed,[32] the truncated morphology transforms into a lozenge as the {100} sectors become narrower along the *a* axis. Insets in parts b, e, and f are the magnified images of the corresponding enclosed square. Lines in the insets of parts b and e denote the edge of the original lozenge crystal.

during heat treatment of polyethylene single crystals on an HOPG substrate. At about 120 °C (Figure 6b), fine fibrils formed on the crystal surface running roughly perpendicular to the single-crystal edge. Similar fine fibrils were formed when polyethylene single crystals were annealed on Si substrate[26,27] and when normal alkane $C_{60}H_{122}$[24] and ultralong alkane $C_{390}H_{782}$[27] were heated on HOPG. Fine fibrils become ordered in these alkane crystals on annealing, encountering with an angle of 120 or 60°. Here, a texture like a vein of a leaf was formed. Fibrils are oriented in the texture in a different way among the different sectors. However, the orientational relationship of fibrils with respect to the lateral edge is almost identical independently of the sector. With further heating, the fibrils became longer and extended, exceeding the lozenge edge of the original single crystal, which can be outlined with a lozenge (Figure 6e). As the temperature increased, the fibrils became longer, more ordered, and they were radially closely packed with an axis of 6-fold rotational symmetry about the perpendicular at the center of lozenge single crystal (Figure 6f). On close inspection, it is found that the fibrils are arrayed with a different angle with respect to the sector boundary axes: They encounter at the *a* axis sector boundary at an angle of 120°. The original crystals in Figure 1a differ from those in Figure 5 in that they have the narrow {100} sectors. However, as the 6-fold symmetry holds overall a single crystal, the vein-like texture is not caused by the hexagonal morphological symmetry of truncated lamella at the central part. Of course, single crystals without the {100} sectors exhibited the 6-fold symmetric arrangement of fibrils.

We see from Figure 6 that fibrils extend longer and longer with increasing temperature. Figure 7 shows more clearly the fibrillar-developing phenomena with annealing time. At the beginning, when polyethylene single crystals were brought up at 132 °C (Figure 7a), a vein-like fibrillar texture formed. After the single crystals were kept for 20 min at the temperature, finer fibrils grew out over the edge from the tips of the thus formed fibrils. When the single crystales were kept longer at the temperature, the newly grown fine fibrils extended further. Similarly, fine fibrils were developed from the edge of ultralong alkane $C_{390}H_{782}$ single crystals on annealing.[27] It is noteworthy here that the fine fibrils do not always extend in the same direction as that of long axes of parent fibrils in the original polyethylene lamella.

E. On Uniaxially Oriented Isotactic Polypropylene. Polyethylene single crystals were rather rapidly heated to a temperature above the melting point on an uniaxially oriented iPP film. Figure 8a shows an AFM phase image, which was taken in situ at 145 °C after polyethylene single crystals were heated at the temperature. Polyethylene single crystals were melted down into droplets. When the sample was cooled to 140 °C, fibrils or lamellae on edge were formed in the droplets of molten polyethylene. By cooling further, more fibrils were grown in the droplets. The fibrils are arrayed in an ordered way, making an inclination angle of about 40° with respect to the iPP fiber (molecular) axis (Figure 8b). There are previous reports[33−37] that, when polyethylene is crystallized from the melt on oriented iPP, a crosshatched texture is formed, in which edge-on lamellae are arrayed making an orientational angle of 40° with the iPP axis. Judging from the growth of

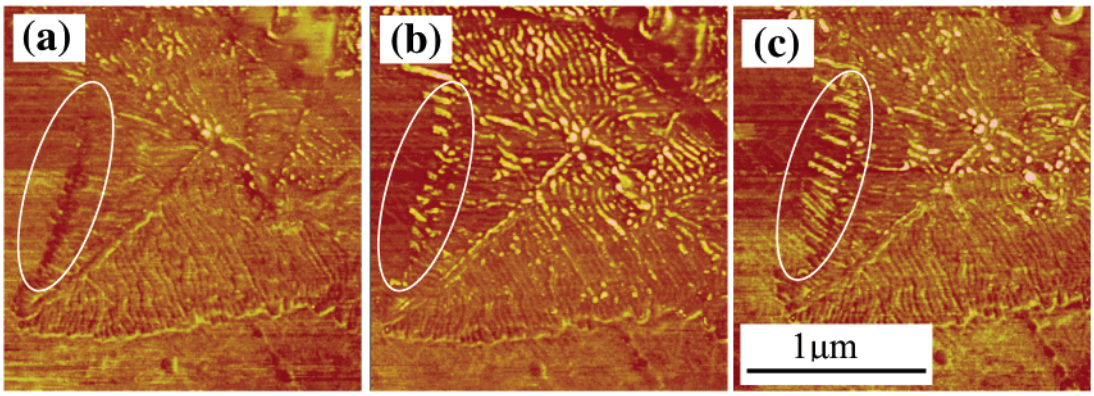

Figure 7. AFM phase images taken in situ on annealing polyethylene single crystals on HOPG at 132 °C at different annealing times: (a) 5, (b) 20, and (c) 60 min. The width of fibrils in the enclosed area ranges from 45 to 50 nm, and from 35 to 40 nm around the central area where fibrils are packed compactly in part c. Fibrils in the enclosed area with the ellipse extend from about 180 to 200 nm, as an average, with increasing time of 5 (a) to 60 min (c).

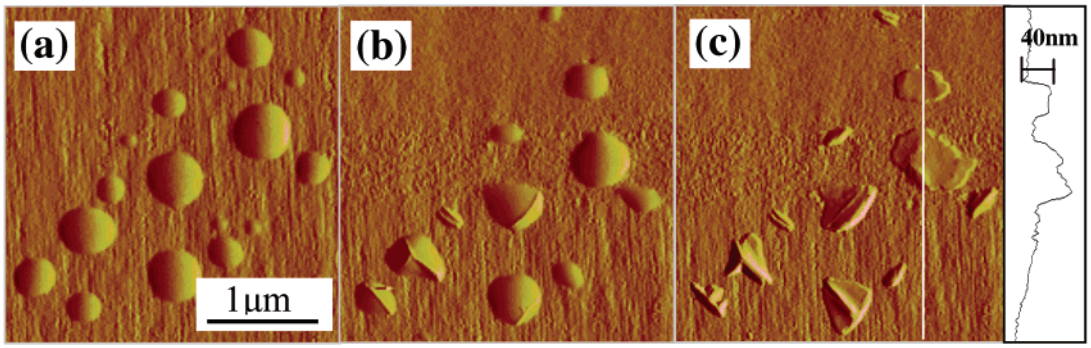

Figure 8. AFM amplitude images taken in situ at (a) 145, (b) 140, and (c) 136 °C on cooling of polyethylene melt on the uniaxially oriented iPP film. The molecular axis of iPP is vertical. The height profile in part c was scanned along a white line. The thickness of the flat-on crystal is 40 nm.

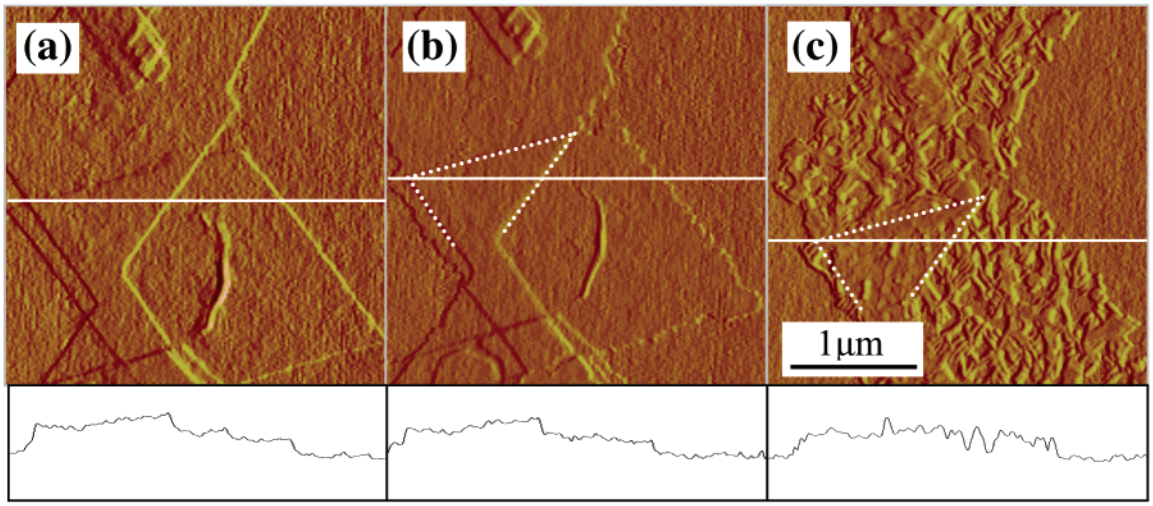

Figure 9. AFM amplitude images taken at various temperatures on annealing of polyethylene single crystals on the uniaxially oriented *i*PP film: (a) room temperature, (b) 125 °C, and (c) 146 °C. These images were recorded after 40 min since being heated to the temperatures. The iPP molecular axis is vertical. The profiles were obtained by scanning along the line of corresponding image. In the profile in part c, the thickness of "the melt" of stacked lamellae is identical to that of the single-layered lamella.[38]

present fibrils from the melt, we see that their morphology is basically similar to the crosshatched structure; lamellae grew edge-on but were singly oriented. Figure 8c shows an AFM image taken in situ at 136 °C during cooling. Flat-on lamellae also grew with a thickness of 40 nm. The whole morphology of Figure 8c did not change on cooling to room temperature.

Figure 9 shows a series of AFM amplitude images that were taken in situ at the described temperatures while the temperature was increased stepwise. That is, an image was recorded at a temperature in the temperature range of 120−146 °C—it took about 5 min per image—and subsequently, the temperature was increased by 2 °C. This process was repeated until 146 °C was reached. In Figure 9b, the rim of a single-layered but not overlapping lamellar single crystal is serrated. The morphological changes again occurred at the periphery. The growth of fine fibrils started at about 130 °C within single crystals, but not within the overlapping lamella whose original shape was still retained (see the

Table 1. Contact Angle of Polyethylene Melt on Various Substrates

substrate	glass	amorphous carbon	evaporated Pt/Pd	HOPG	uniaxially oriented iPP
contact angle (deg)	15−31	3−8	5−10	12−22	18−24

enclosed area in Figure 9c).[10,17] With increasing the temperature, a fine textural structure was developed. Fine fibrils were oriented in two directions with the same inclination angle and maybe woven into a crosshatched texture. In the texture, fibrils are preferentially oriented at an angle of about 40° with respect to the fiber axis of iPP (discussed in detail later). When polyethylene single crystals were heated rather quickly to a temperature above the melting point as in Figure 8, droplets of melt were caused. In contrast, as shown in Figure 9c, the crosshatched morphology of the "polyethylene melt" was still retained when polyethylene crystals were heated stepwise above the melting point. In comparing the morphological changes in Figures 8 and 9, it is found that the melt morphology produced on the substrate depends on the rate of heating.

Discussion

We see above that the polyethylene melt behaves differently on different kinds of substrates. From the height profile as in Figure 4b, the contact angle of polyethylene melt on Pt/Pd can be measured. (Since the profile goes up steeply to the substrate at the edge, it seems the contact angle should be large; however, note that the axis units of the ordinate and abscissa are largely different.) The contact angles thus measured for various substrates with the polyethylene melt are listed in Table 1. Since molten polyethylene does not expand over the Pd/Pt substrate surface, it is considered that the interfacial free energy should be large. In fact, the contact angle is small. However, the contact angle on glass plate, i.e., another inorganic substance, is large. Although evaporated carbon and HOPG have a chemically identical constitution, the contact angle largely differs between the two substrates. Evaporated carbon is amorphous and consists of mosaics. In contrast, HOPG has a smooth surface in which carbon atoms are arranged regularly. Considering these results, we notice the following: "evaporated" substances, which are mosaic or polycrystalline, have a smaller contact angle, while in contrast, a continuous surface, e.g. glass plate and HOPG, has a larger contact angle. However, the contact angle on iPP is large, although polycrystalline.

During annealing, thickening initiated at the periphery of single crystals. The periphery is more unstable due to the excess of lateral surface free energy, thinner or with more defects, and hence partial melting takes place there when polyethylene single crystals are heated: the "molten state" could be produced transiently. The transiently molten polyethylene cannot flow away on the substrate because it might be still highly viscous at the annealing temperature. The transiently produced polyethylene melt could stay there and soon recrystallize with a larger thickness. Thus, a framelike feature can result. The thicker crystallites remain stable in some range of temperature above the recrystallization temperature, and hence reorganization followed inside the framed lamella with further heating. This explains the temperature dependence of lamellar thickness at the periphery and inside lamellae on annealing on a glass plate, as shown in Figure 2. Of course, since the morphology depends on the annealing time, the thickness become uniform over the whole lamellae when they are left longer at a fixed temperature.

Before single crystals melt on glass plate and amorphous carbon, notches are generated at the periphery and extended with a raised edge, to carve into the interior of lozenge crystal. On Pt/Pd, polyethylene single crystals behave in a morphologically different way by annealing. When polyethylene crystals, which normally have a hollow pyramidal shape in solution, are dried up on a substrate, they collapse. It is unlikely that the collapsed morphology differs among the different kinds of substrates. Thus, it is unlikely that the different morphological behaviors of polyethylene single crystals observed by annealing could be due to the morphological difference in collapsed lamellae at room temperature. The affinities between polyethylene crystals and substrate should be different at high temperatures.

The polyethylene melt forms semisphere droplets on both evaporated carbon and HOPG. However, in the heating process until polyethylene single crystals melt out, they behave quite differently between the two substrates. Though consisting of only carbon, the two have different surface structures: Since evaporated carbon film is amorphous and consists of mosaic blocks, carbon atoms are randomly arranged on its surface, and in contrast, HOPG comprises stacked layers, on the exposed surface of which carbon atoms are ordered hexagonally. It is clear that the difference in annealing behavior between the two kinds of substrates should be caused by the difference in their surface structure: On HOPG, epitaxial adjustment of polyethylene crystals to substrate can be performed.

Figure 10 shows a deformed appearance of polyethylene lamella at an early stage of annealing on HOPG. Thickness decreases around the lamellar edge by growth and extension of fine fibrils from there. Reorganization occurs at a low temperature of 100 °C. However, no fibrils are formed in the lamellar interior. Figure 2 shows that the thickness decreases at the edge. In contrast, thickening takes place at the periphery on evaporated carbon (Figure 5c).

As seen in Figure 6, a texture like a leaf vein, consisting of fibrils, is organized in the single crystals by annealing on HOPG. In the annealing process, order increases with increasing annealing temperature, and eventually the fibrils are arrayed radially from the center of polyethylene single crystal and packed with an axis of 6-fold rotational symmetry at the center (Figure 6f). The dexterously assembled fibrillar texture within single crystals is characteristic of annealing on HOPG: fibrils in the sectors on both sides of the *a*-axis sector boundary encounter one another at an angle of 120° at the boundary, but they do not always impinge against the boundary at a half of the encounter angle, i.e., 60°. When polyethylene single crystals were annealed in suspension in an inert media, holes were formed and extended almost perpendicular to the {110} lateral surfaces, and notches initiated at the periphery were also extended toward the interior of lamella in the same direction.[10] As a result, fibrils perpendicularly oriented to the {110} surfaces were formed. It seems to be essential that fibrils should be produced on annealing polyethylene single crystals without the effect of sub-

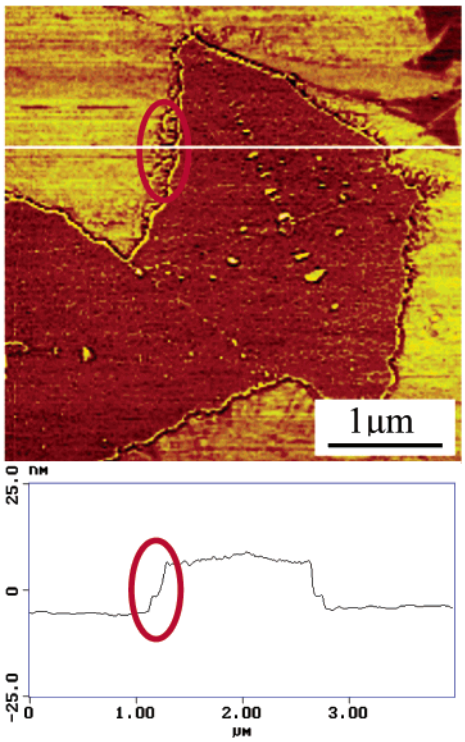

Figure 10. AFM height image taken in situ on annealing polyethylene single crystals on HOPG at 100 °C, and height profile corresponding to a line in the image. Fine fibrils grow from the periphery.

strate and oriented perpendicularly to the side surface. The orientational relationship of fibrils to the lamellar side surface appears to hold in present annealing on HOPG. It is thus considered that when the thus perpendicularly oriented fibrils extend toward the *a* axis sector boundary in the adjacent sectors, they could encounter at the boundary at about 120°. In other words, it is suggested that the hexagonal rotational symmetric array of fibrils at the center of lamella could be induced in this way, irrespective of the orientational relationship between single crystal and the substrate. However, some observations demonstrate that the 120° orientational relationship among fibrils is performed *on HOPG*: alkane crystals epitaxially grow;[39] melt-grown polyethylene lamellae were aligned with their long axis parallel to the HOPG surface and oriented at every 120°;[40,41] the long chain alkane ribbons or fibrils were formed and aligned in three main directions on annealing, showing an overall hexagonal ordering.[24,27] On the other hand, fibrils are not arrayed orderly on the Si substrate.[24,27] On the basis of these observations, it is properly concluded that the veinlike texture should be induced under epitaxial influence by the HOPG surface. So far, there have been reported a large number of epitaxial systems concerning polymers, which occurred from melt and from the solution on various organic and inorganic substances.[42−43] Here, it is emphasized that the epitaxial orientation can be also performed *through partial melting in the annealing process before melting*. The extension of finer fibrils, which are grown at the periphery, could be driven by the epitaxial mechanism. Here, there are three important inquiries about the fibrils: (1) How do fibrils form in the single crystals? (2) What is the fibrillar structure? (3) Why do the fibrils orient differently among sectors? As for the last, it is

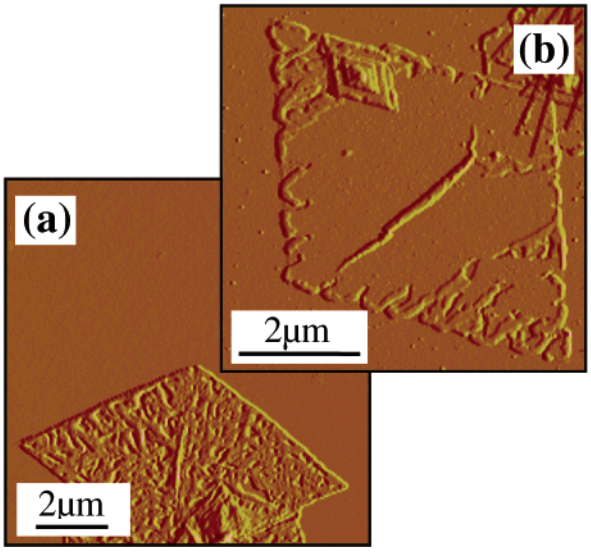

Figure 11. AFM phase images taken in situ at an early stage of annealing of polyethylene single crystal: (a) after 5 min at 120 °C on a glass plate and (b) after 5 min at 122 °C on evaporated carbon.

suspected that the folding direction of chains differs among sectors.

Figure 7 shows that the morphology of polyethylene single crystals changes with time during annealing on HOPG at a given temperature. It is well-known from previous reports that when polyethylene single crystals are annealed, many small holes are formed over the whole area. No small holes are seen in Figure 1c. At an early stage of annealing, small holes are, in fact, observed in the present annealing on the glass plate (see Figure 11a). Small holes were also formed at the initial annealing on amorphous carbon substrate.[9,17,26] On further annealing, a lamella is carved deeply along the *b* axis as seen in Figure 11b with raised edges.[17,27] On annealing in inert medias, holes extend in the ⟨130⟩ direction even in the lamellar interior.[10] Holes produced at the initial stage of annealing are combined, and small, separated crystalline domains are fused into a continuous lamella, leaving a small number of large holes; it is the same phenomenon as small water droplets condensing into larger ones with time. This may be the basic mechanism of the so-called amoeba-like motion.[7,31] Figure 12 shows another process in which the morphology changed with time during annealing: A net texture is developed by longer annealing.

On the oriented iPP film, fine fibrils grew in the process of stepwise annealing, preferentially oriented with a fixed inclination angle in one direction or in the crossed way, as seen in Figure 9. When polyethylene is crystallized from the melt on the oriented iPP film, the crosshatched texture is organized, as seen in Figure 13. In Figure 13, the lamellae on edge make an angle of 40° with the iPP fiber axis. The textural formation is well-understood by the epitaxial mechanism;[33−36] $(100)_{PE}$// $(010)_{iPP}$, $[001]_{PE}$//$[101]_{iPP}$. (name mode I). In Figure 9c, the long axes of fibrils are also oriented at an angle of about 40° with the iPP fiber axis. In Figure 12, we can see that, during annealing, fibrils are formed and are in the process where they are arrayed in the above orientation although poorly ordered. Figure 14 shows the electron diffraction pattern of a specimen in which polyethylene exhibited a networklike polyethylene texture like that in Figure 12c. The electron diffraction

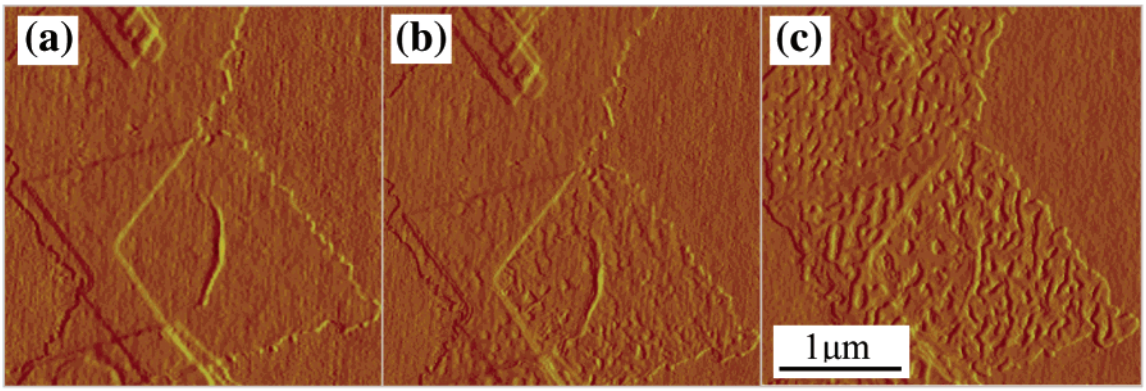

Figure 12. AFM amplitude images taken in situ at 130 °C at (a) 5, (b) 20, and (c) 60 min on annealing on iPP substrate. The iPP molecular axis is vertical.

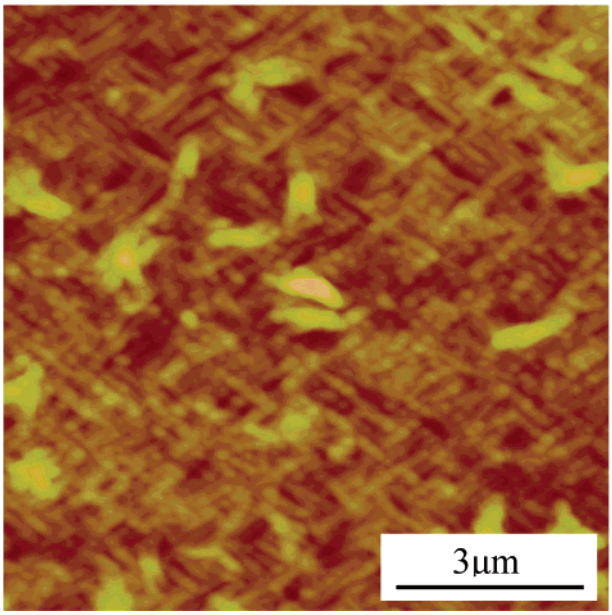

Figure 13. AFM height image of polyethylene crystallized from the melt on the uniaxially drawn iPP film. The iPP molecular axis is horizontal.

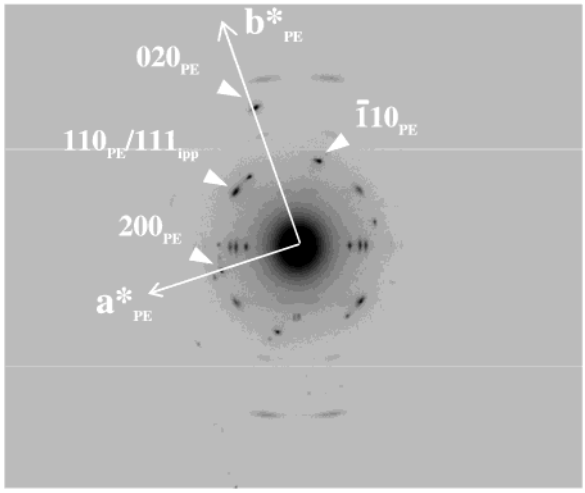

Figure 14. Electron diffraction pattern of the uniaxially drawn, thin iPP film on which polyethylene single crystal was annealed at 132 °C for 60 min. The iPP molecular axis is vertical.

pattern from polyethylene crystals is not the fiber pattern given rise to by the melt-grown, crosshatched texture,[36] but like that of a single-crystal pattern.

The electron diffraction pattern from polyethylene in Figure 14 is surely similar to an *hk*0 net pattern of single crystal. It is characteristic that the 110 diffraction spot of polyethylene is coincident with the 111 reflection of iPP fiber pattern. The electron diffraction pattern resembles quite well that of Figure 5a in ref 44; alkane single crystals grow flat-on from the melt, giving an *hk*0 net pattern in which the 110 spot coincides with the iPP 111 reflection. This implies that the molecular orientation in Figure 14 should be understood based on the same epitaxial model as described in ref 44. However, the coincidence of the PE 110 reflection and iPP 111 one is an apparent event in the diffraction phenomenon and not essential for the overgrowth mechanism. In reality, as seen from the mechanism of PE/iPP epitaxy resolved by Wittmann and Lotz,[34,35] the iPP (010) plane is also attributed to the oriented overgrowth of alkane on iPP substrate. According to the overgrowth mechanism proposed by them,[35] three modes are possible for the epitaxy of alkane on iPP and that of PE on iPP: (1) $(001)_{para}//(010)_{iPP}$, $[\bar{1}10]_{para}//[\bar{1}01]_{iPP}$, (2) $(001)_{para}//(010)_{iPP}$, $[110]_{para}//[\bar{1}01]_{iPP}$, and (3) $(001)_{para}//(010)_{iPP}$, $[100]_{para}//[101]_{iPP}$, where the suffix para stands for alkane or polyethylene. Modes 1 and 2 are in the twin relation with respect to the (110) plane of alkane and polyethylene. In Figure 14, the PE 020 reflection is observed at an angle of about 17° with the iPP fiber axis anticlockwise and the 110 reflection at about 13° clockwise. (In the case of epitaxy of alkane on iPP (cf. Figure 5 in ref 44), the angular relationship of 020 and 110 reflections hold also). The orientational relationship of the PE 020 and 110 reflections proves that the epitaxial mode of 1 actually occurs (named mode II). (In ref 44, the epitaxial mode is expressed as $(001)_{para}//(010)_{iPP}$, $[110]_{para}$ 50° $[001]_{iPP}$. It is crystallographically preferable to define it as above.) Polyethylene chains stand on the iPP surface in mode II while PE chains lay down on it in the mode I, aligning parallel to the [101] direction. In the process of heating, polyethylene single crystals undergo a "transiently molten state," in which molecular chains are not so activated as to be disordered, as in the isotropic melt, i.e., *partial melting*. Keeping their original position within the single crystals in partial melting, molecular chains could be reoriented around their axis, moving through flip-flop motion and/or slide diffusion along their axis. Through the reorganization process, molecular chains are recrystallized to adjust the PE (110) plane with the iPP (101) plane at the in-contact plane.

Concluding Remarks

It was found, from AFM studies, that on annealing, the morphology of polyethylene single crystals changes with increasing time as well as temperature. The melt behavior and morphological features by annealing depend on the kind of substrate, as follows.

(1) The contact angle is smaller on the mosaic and polycrystalline surface, i.e., on evaporated polycrystalline Pt/Pd and evaporated mosaic carbon, than on the continuous, smooth surface such as a glass plate and HOPG, i.e., mosaic and/or polycrystalline surface.

(2) Carbon atoms are arrayed randomly on evaporated carbon, and in a perfectly ordered way on HOPG. The difference in the atomic arrangement on the substrate surface causes the different morphological behaviors during annealing; an epitaxial orientation is induced on HOPG.

(3) The textures were formed within polyethylene single crystals on HOPG and uniaxially oriented iPP in the annealing process: In the partial melting caused by annealing, the single crystals can be reorganized, to give a texture under the influence of the substrate surface, i.e., *epitaxial ordering through partial melting*.

To understand profoundly the annealing behaviors of polymer crystals, it is necessary to study further by taking account of accompanying changes in molecular alignment and orientation.

Acknowledgment. This work was partly supported by a Grant-in-Aid for Scientific Research on Priority Areas: "Mechanism of Polymer Crystallization" (No. 12127207), and partly by the "Nanotechnology Support Project" of the Ministry of Education, Culture, Sports, Science, and Technology, Japan.

References and Notes

(1) Bassett, D. C.; Kerller, A. *Philos. Mag.* **1962**, *7*, 1553−1584.
(2) Holland, V. F. *J. Appl. Phys.* **1962**, *35*, 59−63.
(3) For example: Keller, A. *Rep. Prog. Phys.* **1968**, *31*, Part II, 623−703. Fava, R. A. *J. Polym. Sci., Macromol. Rev.* **1971**, *5*, 1−108.
(4) Geil, P. H. *Polymer Single Crystals*; Wiley-Interscience: New York, 1963.
(5) Wunderlich, B. *Macrmolecular Physics*; Academic Press: New York, 1973.
(6) Bassett, D. C. *Principles of Polymers Morphology*; Cambridge University Press: Cambridge, U.K., 1981.
(7) Hirai, N.; Yamashita, Y.; Mitsuhata, T.; Tamura, Y. *Rep. Res. Lab. Sur. Sci. Okayama Univ.* **1961**, *2*, 1−15.
(8) Fischer, E. W.; Schmidt, G. F. *Angew. Chem.* **1962**, *74*, 551−562.
(9) Nagai, H.; Kajikawa, N. *Polymer* **1968**, *9*, 177−199.
(10) Roe, R.-J.; Gieniewski, C.; Vandimsky, R. G. *J. Polym. Sci., Polym. Phys.* **1973**, *11*, 1653−1670.
(11) Patil, R.; Kim, S.-J.; Smith, E.; Reneker, D. H.; Weisenhorn, A. L. *Polym. Commun.* **1990**, *31*, 455−456.
(12) Snetivy, D.; Vansco, G. J. *Polymer* **1992**, *33*, 432−433.
(13) Reneker, D. H.; Patil, R.; Kim, S.-J. Tsuruk. In *Crystallization of Polymers*; Dosiere, M., Ed.; Kluwer Academic Press: New York, 1992; pp 357−373.
(14) Nakagawa, Y.; Hayashi, H.; Takahagi, T.; Soeda, F.; Ishitani, F.; Toda, A.; Miyaji, H. *Jpn. J. Appl. Phys.* **1994**, *33*, 3771−3774.
(15) Craemer, K.; Wawkuschewski, A.; Domb, A.; Magonov, S. N. *Polym. Bull. (Berlin)* **1995**, *35*, 457.
(16) Winkel, A. K.; Hobbs, J. K.; Miles, M. J. *Polymer* **2000**, *41*, 8791−8880.
(17) Tian, M.; Loos, T. *J. Polym. Sci., Polym. Phys.* **2001**, *39*, 763−769.
(18) de Silva, D. S. M.; Zeng, X. B.; Ungar, G.; Spells, S. J. *Macromolecules* **2002**, *35*, 7730−7741.
(19) Hocquet, S.; Dosiere, M.; Thierry, A.; Lotz, B.; Koch, M. H. J.; Dubreuil, N.; Ivanov, D. A. *Macromolecules* **2003**, *36*, 8376−8384.
(20) Toda, A.; Okamura, M.; Hikosaka, M.; Nakagawa, Y. *Polymer* **2003**, *44*, 6135−6138.
(21) Patil, R.; Reneker, D. H. *Polymer* **1994**, *35*, 1909−1914.
(22) Hobbs, J. K.; Miles, M. J. *Macromolecules* **2001**, *34*, 353−355.
(23) Ivanov, D. A.; Amalou, Z.; Magonov, S. N. *Macromolecules* **2001**, *34* (26), 8944−8952.
(24) Magonov, S. N.; Yerina, N. A. *Langumuir* **2003**, *19*, 500−504.
(25) Hobbs, J. K. In *Polymer Crystallization*; Sommer, J.-U., Reiter, G., Eds.; Springer-Verlag: Heidelberg, Germany, 2003; Chapter 7, pp 82−97.
(26) Ivanov, D. A.; Magonov, S. N. In *Polymer Crystallization*; Sommer, J.-U., Reiter, G., Eds.; Springer-Verlag: Heidelberg, Germany, 2003; Chapter 7, pp 98−130.
(27) Magonov, S. N.; Yerina, N. A.; Ungar, G.; Reneker, D. H.; Ivanov, D. A. *Macromolecules* **2003**, *36*, 5637−5649.
(28) Blundell, D. J.; Keller, A.; Kovacs, A. I. *Polym. Lett.* **1966**, *4*, 481−486.
(29) Petermann, J.; Gohil, R. M. *J. Mater. Sci.* **1979**, *14*, 2260−2263.
(30) Statton, W. O.; Geil, P. *J. Appl. Polym. Sci.* **1960**, *3*, 357−361.
(31) Nirai, N. In ref 4, p 326.
(32) Kawaguchi, A.; Ohara, M.; Tsuji, M. *J. Polym. Sci., Part B: Polym. Phys.* **1994**, *32*, 421−436.
(33) Lotz, B.; Wittmann, J. C. *Macromol. Chem.* **1984**, *185*, 2043−2052.
(34) Lotz, B.; Wittmann, J. C. *J. Polym. Sci. Polym. Phys.* **1986**, *24*, 1541−1558.
(35) Lotz, B.; Wittmann, J. C. *J. Polym. Sci. Polym. Phys.* **1986**, *24*, 1559−1575.
(36) Petermann, J.; Broza, G.; Rieck, U.; Kawaguchi, A. *J. Mater. Sci.* **1988**, *22*, 1477−1481.
(37) Lee, I.-H.; Schultz, J. M. *J. Mater. Sci.* **1988**, *23*, 4237−4243.
(38) Loos, I.; Koemen, J.; Dchmidt, U. Application Note; Molecular Imaging Corp.: Phoenix, AZ, 2000.
(39) Boucher, E. A. *J. Mater. Sci.* **1973**, *8*, 146−148.
(40) Baukema, D. A.; Hopfinger, A. J. *J. Polym. Sci. Polym. Phys. Ed.* **1982**, *20*, 399−409.
(41) Tracz, A.; Jaszka, J.; Kucviński, I.; Chapel, J.-P.; Boiteux, G. *Macromol. Symp.* **2001**, *169*, 129−135.
(42) Mauritz, K. A.; Baer, E.; Hoffinger, A. J. *J. Polym. Sci., Macromol. Rev.* **1978**, *13*, 1−61.
(43) Wittmann, J. C.; Lotz, B. *Prog. Polym. Sci.* **1990**, *15*, 909−948.
(44) Kawaguchi, A.; Okihara, T.; Ohara, M.; Tsuji, M.; Katayama, K. *J. Cryst. Growth* **1989**, *94*, 857−870.

MA0498666